SF2A 2024
M. Béthermin, K. Baillié, N. Lagarde, J. Malzac, R.-M. Ouazzani, J. Richard, O. Venot, A. Siebert (eds)

ELECTROMAGNETIC FOLLOW-UP DURING THE LISA MISSION

P.-A. Duverne[1], F. Cangemi[1], A. Coleiro[1], S. Marsat[2], R. Mignon-Risse[1,3] and P. Varniere[1]

Abstract. The LISA mission is due to start in the mid-2030s and will be observing low-frequency gravitational waves (GW). At the same time, the ATHENA mission will be monitoring X-ray sources at an unprecedented depth. In that observational context, supermassive binary black hole (SMBBH) mergers constitute an important potential source of multi-messenger observations as they are one of the most promising targets for LISA and could also be detectable in the electromagnetic (EM) regime by ATHENA. In this contribution, we present a simulated population of GWs observed by LISA before the merger and the associated localisation uncertainties. Based on those simulations, we used several electromagnetic emissions models to simulate realistic follow-up campaigns with two instruments: LSST and ATHENA. The former helps with tracking the time evolution of the circumbinary disk of SMBBH approaching the merger. The latter provides insights into the evolution of the mini-disks located around each of the two component masses of the binary.

Keywords: LISA, gravitational waves, ATHENA, LSST, multi-messenger astronomy, supermassive black hole, accretion

1 Introduction

In 2017, the gravitational wave (GW) GW170817 (Abbott et al. 2017) was detected by LIGO and Virgo along with various electromagnetic (EM) counterparts across the whole spectrum (LIGO Scientific Collaboration et al. 2017). This joint detection opened a new era for astronomy, providing new ways of probing the violent universe. However, the recent observing runs of LIGO and Virgo, such as O3 (2019-2020) and O4 (2023-present), showed the inherent observational difficulties of such multi-messenger observations: the need for coordination between the different observatories/instruments and the large quantity of observing time to find counterparts are two of the most prominent ones (Antier et al. 2020). Henceforth, for this work, we try to explore the observational constraints that multi-messenger astronomy will face in the future with the start of the new GW detectors.

In the next decade, the LISA satellite (Amaro-Seoane et al. 2017) will be launched and detect low-frequency GW in the [0.1, 100]mHz band. The supermassive black hole binaries (SMBBH) coalescences, which are expected to happen after the mergers of their host galaxies, are one of the most promising sources for LISA. Even though the black hole components are not photon emitters themselves, the local surroundings of the binary is a rich and complex mixing of matter that is bright over the whole EM spectrum. Consequently, SMBBH are also good candidates for multi-messengers observations (Bogdanović et al. 2022, and references therein). In particular, the emissions in the optical wavelengths and in the X-ray domains make SMBBH targets for instruments such as, respectively, LSST-VRO (LSST Science Collaboration et al. 2009) or the upcoming NewATHENA satellite McGee et al. (2020); Piro et al. (2022). Joint observations of those binaries would yield important results in several domains, such as cosmology, by providing a new estimate of the Hubble constant H_0. It would also provide new tests of the General Relativity theory or constrain the accretion-ejection processes in the binary environment. For this work, we identify the most promising cases for pre-merger detection of GW emitted by SMBBH and follow up with two main EM instruments: VRO-LSST in the optical domain and ATHENA for the X-rays.

We start by describing a simulation setup of GW localisation skymaps for a population of SMBBH signals detected by LISA. Then, we describe the model of EM emissions in the optical and X-ray domains. Eventually, we identify the source that are the most easily observable by the EM instruments and LISA.

[1] Université Paris Cité, CNRS, Astroparticule et Cosmologie, F-75013 Paris, France
[2] Laboratoire des 2 Infinis - Toulouse (L2IT-IN2P3), Université de Toulouse, CNRS, UPS, F-31062 Toulouse Cedex 9, France
[3] Department of Physics, Norwegian University of Science and Technology, NO-7491 Trondheim, Norway

2 Gravitational wave observations with LISA

2.1 Simulation setup

For this work, we generated a population of gravitational wave signals emitted by SMBBH sources at several time steps before the merger to produce a sky localization of LISA and identify the best candidates for multi-messenger observations. LISA sensitivity band is in the interval [0.1, 100]mHz, which allows to detect SMBBH in the range of total masses $[10^4, 10^7]$ $M_\odot$. Consequently, we use representative total masses M_{tot} in the set $\{10^4, 10^5, 10^6, 10^7\}$ $M_\odot$ and mass ratio q in $\{1, 3, 10\}$. For each couple (M_{tot}, q), we simulate 500 signals. The signals are evenly distributed in volume in a shell with inner and outer radiuses of 500 Mpc and 20,000 Mpc, respectively, corresponding to the horizon of LISA (Amaro-Seoane et al. 2017). The aligned component spins are evenly distributed in [-1, 1]. The various angles are chosen uniformly in $[0, 2\pi]$, except for the angle between the angular momentum and the line of sight (i.e. the inclination ι) whose *cosine* is chosen uniformly in [-1, 1].

For each signal, we run the LISABETA algorithm (Marsat et al. 2021) that uses a Bayesian approach to perform parameter inference on the GW signals. Among the inferred parameters, we isolate the right ascension, the declination and the luminosity distance posteriors, obtained by marginalizing over the other parameters. We will refer to this quantity as the *skymap* for simplicity. LISABETA includes the three phases of the merger - inspiral, merger and ringdown - and uses the higher-order modes of the GW signals, allowing to break degeneracies in the posterior distributions. The posterior can still present multi-modalities in the sky, caused by the LISA instrument triangular configuration symmetries, but those are typically reduced post-merger to a bi-modality at worst, making the EM follow-up easier (Marsat et al. 2021).

2.2 Localisation results

After the inference, the skymaps are generated using the HEALPIX formalism to project the posterior on the sky. It also allows to extract the size of the localization contours. Figure 1 shows the distribution of the 90% credible region (CR) area for the populations described in Section 2.1. The points correspond to the median of the CR area distribution at the different time steps and the error-bars to the 90% interval. As expected from previous studies (Piro et al. 2023; Mangiagli et al. 2022), the CR area shrinks over time as the GW signal becomes stronger in LISA, and the signal-to-noise ratio (SNR) accumulates in the data. The total mass is also a parameter that influences the CR area size. For the heaviest SMBBH with $M_{tot}=10^7$ $M_\odot$, the CR is significantly larger than the rest of the population. The mass ratio has little influence on the skymap size. The significantly larger areas for the ($M_{tot}=10^4$ $M_\odot$, q=1) case is due to a likely convergence issue in LISABETA that is still under investigation. Regardless, even as close as six hours before the merger, the localization area reaches the 100 deg^2 level for the light SMBBH of the population. Such localizations are highly demanding in observing time. Hence predicting the EM emission connected to SMBBH mergers is necessary for optimizing the follow-up.

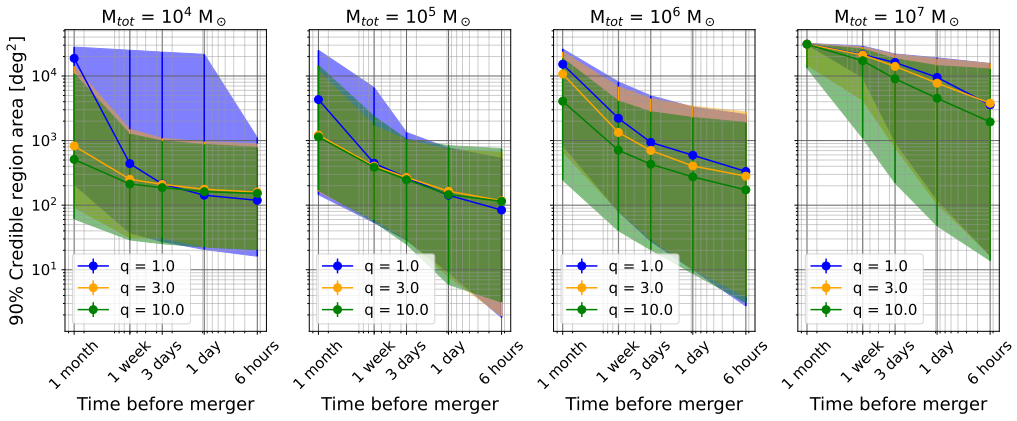

Fig. 1: Localisation areas of the 90% CR for the population of GW signals described in Section 2.1.

3 Electromagnetic follow-up

Based on the recent advancements in GRMHD (Gutiérrez et al. 2024, and references therein), the surrounding of an SMBBH close to the merger comprises five components. The *circumbinary disk* (CBD) is the accretion disk around the binary, the *mini-disks* (mDs) are two accretion disks around each black hole component, the *cavity* that is a low-density space between the CBD and the mDs created by the orbital motion of the black holes, two *gaz streams* that accrete matter from the CBD onto the mDs and an over-density located in the innermost region of the CBD, called the *lump*. As they are electromagnetically bright, two components are of particular interest in our case: the CBD and the mDs. The CBD emits primarily in the optical band for the LISA targets. The mDs being hotter, they are X-ray bright. Consequently, they both are good follow-up candidates with respectively LSST-VRO and ATHENA.

3.1 Electromagnetic model

We use two emission models to estimate the detectability of the CBD and the mDs. We model the emission of the CBD with a multi-colour black-body spectrum as it would be done for the accretion disk of a single black hole (Shakura & Sunyaev 1973; Mitsuda et al. 1984; Makishima et al. 1986), but truncated. The spectrum is calculated with a truncation radius estimated to be twice the orbital separation (Mignon-Risse et al. 2024) at the different time steps before the merger detailed in Section 2.1. For Figures 2a and 2b, the results are shown three days before the merger.

On the X-ray side, we use a Doppler shift model from Dal Canton et al. (2019), where the lightcurve of the mDs is modulated by the orbital motion of the two black holes at the same frequency as the GW. This model allows us to estimate which SMBBH is observable but also provides a means to identify that the observed object is actually an SMBBH. Otherwise, confirming that the observed source is a close-to-merger binary is complex.

3.2 Electromagnetic observability

Using the models described in Section 3.1, we try to identify the most observable SMBBH binaries. For the optical part, we use LSST-VRO as the observing instrument and based on the model described in the previous section, we correlate the spectrum with the r filter passband to estimate the object's magnitude. Then, we define two criteria for an SMBBH to be detectable for a joint detection LISA/LSST-VRO: the GW localisation area has to be less than 150 deg^2 for it is the typical size of the pre-merger localisation, as visible in Figure 1 and an area that LSST-VRO can reasonably cover in a night of observation with its 9 deg^2-field of view (FoV). The second criterion is that the LSST-VRO magnitude has to be less than 24 mag, which roughly corresponds to the expected depth of a single image. We use ATHENA and its Wield Field Imager (WFI) as it has a large FoV of 0.4 deg^2 as the preferred observatory for the X-ray observations. For simulating an observation with the latest response files *. We then estimate the SNR, assuming a Poisson distribution for the noise. As the detection of the time variabilities is crucial for identifying the SMBBH, we define a parameter $\alpha = \tau \times f_{GW}$, where τ is the exposure time necessary to reach and SNR of 5 in WFI and f_{GW} is the frequency of the GW at the time of the observation. Using the Shannon theorem, the signal variabilities can be detected when $\alpha < 1/2$. Figure 2a shows the r magnitude for the population of the (M_{tot}=10^5 $M_\odot$, q=10) (hexagon) and (M_{tot}=10^7 $M_\odot$, q=10) (squares), and the hatched region correspond to the multi-messenger observability region we previously described. The two populations in the plot are outside the observability region, but each for distinct reasons. The light SMBBH have a CBD too faint to be detectable by LSST-VRO but are reasonably localised with LISA. In contrast, LISA poorly localises the heavy ones to be easily identifiable, but their CBD is bright enough to be observed by LSST-VRO. Figure 2b shows the distribution of the α parameter for the whole population of SMBBHs. The only population for which the modulations can be detected are the 10^7 $M_\odot$ binaries, with the same caveat as previously about the LISA localisation. Both optical and X-rays demonstrate that there will be a compromise to find between the interesting targets for GW detection, that are the light SMBBH, based on Section 2.2 and Figure 1, and the EM-detectable source.

*https://www.mpe.mpg.de/ATHENA-WFI/response_matrices.html

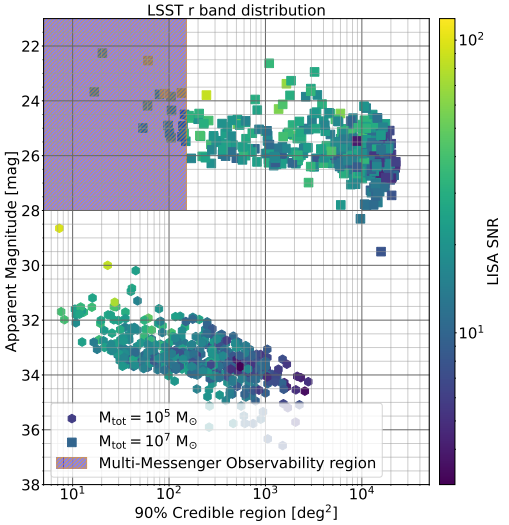

(a) r band LSST magnitudes for the CBD spectrum. The squares corresponds to the M_{tot}=10^5 $M_\odot$ population and the hexagons to the M_{tot}=10^4 $M_\odot$ SMBBH.

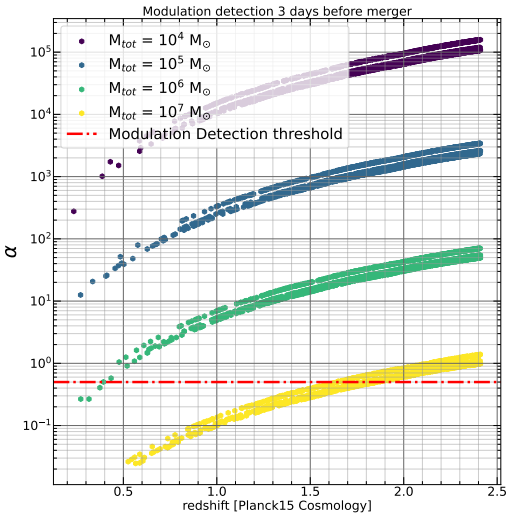

(b) α parameter for the whole SMBBH population, three days before merger and the red, dashed line is the threshold for modulation detection.

4 Conclusions

For this work we simulated a population of GW signal emitted by SMBBH binaries and detected before the merger by LISA. We associated EM models for the CBC and mDs of these sources, which correspond to optical and X-ray emission. Then, we identify the cases most likely to be observed via GW and photons. The main result of this work is that the best cases for GW detection and localisation are the light SMBBH, with $M_{tot} \sim 10^4 - 10^5\ M_\odot$. On the contrary, the best candidates for EM observations are the heaviest SMBBH, both in brightness and variabilities detectabilities. These observations point toward a compromise between what is easily GW observable and what is EM observable.

This work was supported by the Programme National des Hautes Énergies (PNHE) of CNRS/INSU co-funded by CNRS/IN2P3, CNRS/INP, CEA and CNES. We thank the IT support of UPC for providing us with computing ressources on the DANTE cluster.

References

Abbott, B. P., Abbott, R., Abbott, T. D., et al. 2017, Phys. Rev. Lett., 119, 161101
Amaro-Seoane, P., Audley, H., Babak, S., et al. 2017, arXiv e-prints, arXiv:1702.00786
Antier, S., Agayeva, S., Almualla, M., et al. 2020, MNRAS, 497, 5518
Bogdanović, T., Miller, M. C., & Blecha, L. 2022, Living Reviews in Relativity, 25, 3
Dal Canton, T., Mangiagli, A., Noble, S. C., et al. 2019, ApJ, 886, 146
Gutiérrez, E. M., Combi, L., & Ryan, G. 2024, arXiv e-prints, arXiv:2405.14843
LIGO Scientific Collaboration, Virgo Collaboration, IceCube Collaboration, et al. 2017, APJL, 848, L12
LSST Science Collaboration, Abell, P. A., Allison, J., et al. 2009, arXiv e-prints, arXiv:0912.0201
Makishima, K., Maejima, Y., Mitsuda, K., et al. 1986, ApJ, 308, 635
Mangiagli, A., Caprini, C., Volonteri, M., et al. 2022, Phys. Rev. D, 106, 103017
Marsat, S., Baker, J. G., & Canton, T. D. 2021, Phys. Rev. D, 103, 083011
McGee, S., Sesana, A., & Vecchio, A. 2020, Nature Astronomy, 4, 26
Mignon-Risse, R., Varniere, P., & Casse, F. 2024, Submitted to MNRAS
Mitsuda, K., Inoue, H., Koyama, K., et al. 1984, PASJ, 36, 741
Piro, L., Ahlers, M., Coleiro, A., et al. 2022, Experimental Astronomy, 54, 23
Piro, L., Colpi, M., Aird, J., et al. 2023, MNRAS, 521, 2577
Shakura, N. I. & Sunyaev, R. A. 1973, A&A, 24, 337